Environmental Science & Technology

Article

pubs.acs.org/est

Primary Gas- and Particle-Phase Emissions and Secondary Organic Aerosol Production from Gasoline and Diesel Off-Road Engines

Timothy D. Gordon,[†,‡,○] Daniel S. Tkacik,[†] Albert A. Presto,[†] Mang Zhang,[§] Shantanu H. Jathar,[†,‡] Ngoc T. Nguyen,[†] John Massetti,[§] Tin Truong,[§] Pablo Cicero-Fernandez,[§] Christine Maddox,[∥] Paul Rieger,[∥] Sulekha Chattopadhyay,[⊥] Hector Maldonado,[#] M. Matti Maricq,[▽] and Allen L. Robinson*[,†]

[†]Center for Atmospheric Particle Studies, Carnegie Mellon University, Pittsburgh, Pennsylvania 15213, United States

[‡]Engineering and Public Policy, Carnegie Mellon University, Pittsburgh, Pennsylvania 15213, United States

[§]Mobile Source Operations, California Air Resources Board, El Monte, California 91731, United States

[∥]Monitoring and Laboratory, California Air Resources Board, El Monte, California 91731, United States

[⊥]Planning and Technical Support, California Air Resources Board, El Monte, California 91731, United States

[#]Research Division, California Air Resources Board, Sacramento, California 95814, United States

[▽]Research and Advanced Engineering, Ford Motor Company, Dearborn, Michigan 48120, United States

Supporting Information

ABSTRACT: Dilution and smog chamber experiments were performed to characterize the primary emissions and secondary organic aerosol (SOA) formation from gasoline and diesel small off-road engines (SOREs). These engines are high emitters of primary gas- and particle-phase pollutants relative to their fuel consumption. Two- and 4-stroke gasoline SOREs emit much more (up to 3 orders of magnitude more) nonmethane organic gases (NMOGs), primary PM and organic carbon than newer on-road gasoline vehicles (per kg of fuel burned). The primary emissions from a diesel transportation refrigeration unit were similar to those of older, uncontrolled diesel engines used in on-road vehicles (e.g., premodel year 2007 heavy-duty diesel trucks). Two-strokes emitted the largest fractional (and absolute) amount of SOA precursors compared to diesel and 4-stroke gasoline SOREs; however, 35−80% of the NMOG emissions from the engines could not be speciated using traditional gas chromatography or high-performance liquid chromatography. After 3 h of photo-oxidation in a smog chamber, dilute emissions from both 2- and 4-stroke gasoline SOREs produced large amounts of semivolatile SOA. The effective SOA yield (defined as the ratio of SOA mass to estimated mass of reacted precursors) was 2−4% for 2- and 4-stroke SOREs, which is comparable to yields from dilute exhaust from older passenger cars and unburned gasoline. This suggests that much of the SOA production was due to unburned fuel and/or lubrication oil. The total PM contribution of different mobile source categories to the ambient PM burden was calculated by combining primary emission, SOA production and fuel consumption data. Relative to their fuel consumption, SOREs are disproportionately high total PM sources; however, the vastly greater fuel consumption of on-road vehicles renders them (on-road vehicles) the dominant mobile source of ambient PM in the Los Angeles area.

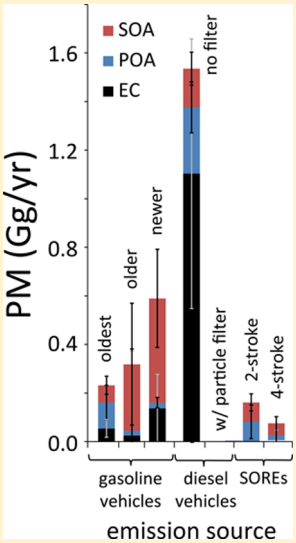

INTRODUCTION

After decades of regulatory focus on reducing on-road vehicle emissions, gasoline and diesel off-road engines are becoming increasingly important sources of air pollutants. Although responsible for only 2% of gasoline consumption, small (<19 kW) off-road engines (SOREs) used in lawn and garden applications (e.g., lawnmowers, leaf blowers, trimmers) emitted 8 million tons of carbon monoxide (CO), nitrogen oxides (NO_x), hydrocarbons (HC), and fine particulate matter ($PM_{2.5}$) in 2007, accounting for 13% of the total U.S. mobile source emissions (excluding commercial air, rail, and marine vessels).[1−3]

While the primary pollutant emissions from off-road engines are known to be high, their contribution to secondary particulate matter (PM) is poorly understood. Secondary PM forms when gas- and/or aqueous-phase oxidation of gas-phase precursors creates low volatility products. When the precursor gases are organic, the secondary PM is referred to as secondary organic aerosol (SOA). Numerous studies have shown that SOA is the largest component of the ambient organic aerosol budget, even in urban areas with substantial primary emissions.[4−6] Recent experiments report significant SOA formation from dilute exhaust from small diesel[7,8] and gasoline

Received: August 9, 2013
Revised: November 21, 2013
Accepted: November 21, 2013
Published: November 21, 2013

engines.[9,10] However, the experiments with gasoline engines did not quantify the SOA formation potential.

This study investigated primary gas and particle emissions from six gasoline SOREs and one diesel transportation refrigeration unit (TRU). The engines included 2- and 4-stroke configurations and a range of sizes (displacements) operated over certification cycles. Dilute emissions from two of the engines were also injected into a smog chamber and then photo-oxidized to quantify secondary PM formation via gas-phase oxidation. Although aqueous-phase oxidation also contributes to SOA production in the atmosphere,[11−14] the experiments were conducted at low relative humidity to reduce experimental complexity. Hence, the SOA formation we report may be a lower bound estimate of SOA production in the atmosphere where both pathways are viable. The research was conducted as part of a large project investigating the link between tailpipe emissions from mobile sources and ambient PM. Companion papers describe primary emissions from on-road vehicles,[15] gas-particle partitioning of POA emissions,[16,17] and SOA formation from on-road gasoline[18] and diesel vehicles.[19]

MATERIALS AND METHODS

Sixteen SORE/TRU experiments were conducted at the California Air Resources Board (CARB) Haagen-Smit Laboratory (HSL) and at Carnegie Mellon University (CMU). These experiments consisted of (a) nine primary-only tests at HSL during which PM and gas emissions were characterized using a constant volume sampling (CVS) system and (b) seven smog chamber tests (three at HSL and four at CMU) during which SOA formation was investigated in a smog chamber. Subsequent sections of this manuscript describe the engines, fuel, test cycles and experimental setup for each of these three categories of tests.

Engines. Six gasoline SOREs used in a variety of applications (backpack leaf blower, soil tiller, string lawn trimmer and lawnmower) and a larger diesel engine for a transportation refrigeration unit (TRU) were tested; engine details are provided in Table S.1 of the Supporting Information (SI). The SOREs included both 2- and 4-stroke engines manufactured between 2002 and 2006. Most of the engines had seen little or no use, as they were purchased by CARB for test purposes only. The TRU engine was older (1998) and had been in service for >1000 h. All of the engines met the relevant certification standard (Title 13, California Code of Regulations, (13 CCR) Section 2403(b)). None of the engines was equipped with a catalyst or other aftertreatment device to reduce emissions. The engines were not chosen to represent the diverse fleet of in-use SOREs and TRU engines, but to screen emissions from a range of technologies.

Fuels and Test Cycles. The same California commercial summertime gasoline was used in all the SORE tests. A commercial ultralow sulfur diesel fuel was used for the TRU testing. Fuel property data are in Table S.2 of the SI. The same commercially available 2-stroke oil was used in all 2-stroke experiments.

For primary-only testing, the engines were operated on an engine dynamometer following CARB procedures for engine certification (http://www.arb.ca.gov/regact/sore/test_fin.pdf) which are based on SAE J1088. The test cycles depend on engine size and application; they are listed in Tables S.1 and S.3 of the SI. Briefly, each test cycle consists of two to six separate phases or modes during which the engine is operated at a specified speed and load. Prior to testing, each engine was warmed up by operating it for 20 min at 50% load.

For the smog chamber experiments, the engines were not operated with an engine dynamometer. Instead they were installed in leaf blowers, which provided the load. They were operated following the 2-mode C test cycle—full throttle for 85% of the test period and idle for 15%. Emissions were added to the chamber over the entire C test cycle; thus, these experiments represent cycle average emissions.

Primary Emissions Characterization. Figure S.1 of the SI shows a schematic of the experimental set up. For the experiments conducted at HSL, the entire raw exhaust was sampled through a custom-fabricated stainless steel inlet into a constant volume sampler (CVS) following the procedure outlined in the Code of Federal Regulations Title 40 Part 8. The CVS was operated at a combined (dilution air plus exhaust) flow rate of between ∼350 ft^3/min and 1000 ft^3/min, depending on the expected emission level of the engine. The primary emissions were determined from samples drawn from the CVS.

Gaseous emissions of carbon monoxide (CO), carbon dioxide (CO_2), methane (CH_4), nitric oxide (NO), nitrogen oxides (NO_x), and organic gases were measured using an AVL-AMA 4000 test bench. Emissions of speciated C_2 to C_{12} hydrocarbons were determined by gas chromatography with flame ionization detection of diluted exhaust samples collected in Tedlar bags (http://www.arb.ca.gov/testmeth/slb/sop102-103v2-2.pdf). Emissions of carbonyls were determined from samples collected on 2,4-dinitrophenylhydrazine (DNPH) impregnated cartridges that were analyzed by high-performance liquid chromatography (HPLC) with an ultraviolet (UV/vis) detector (http://www.arb.ca.gov/testmeth/slb/sop104v3.pdf). Gaseous emissions were corrected for background pollutant concentrations measured in the filtered dilution air immediately downstream from the CVS HEPA filters.

Details of the CVS PM sampling and analysis are provided in the SI.

Smog Chamber Experiments. Smog chamber experiments were conducted at both HSL and CMU to quantify SOA formation from the dilute emissions from two of the SOREs (Table S.1 of the SI). For the HSL experiments, dilute emissions were drawn off of the CVS using a heated (47 °C) Silcosteel treated (i.e., passivated) stainless steel tubing into a 7 m^3 Teflon smog chamber following the approach of Miracolo et al.[20] For the CMU experiments, the emissions were transferred directly from the engine exhaust system into a 10 m^3 Teflon chamber following the approach of Grieshop et al.[21] Before the addition of exhaust, the chambers were partially filled with HEPA- and activated-carbon filtered air. After filling, the exhaust in the chamber was about 200 times more dilute than at the tailpipe.

After adding exhaust, nitrous acid (HONO) was bubbled into the chamber as a hydroxyl radical (OH) source, and VOC:NO_x ratios were adjusted by adding either propene (in experiment SORE4S-4.1) or NO (in experiment SORE2S-1.2) to the chamber. In every experiment except SORE2S-1.1 the VOC:NO_x ratios were between 1.3 and 5.2 (SI Table S.6). In 5 of the 7 chamber experiments between 0.06 and 0.10 ppm of deuterated butanol was injected into the chamber to serve as a hydroxyl radical tracer. After ∼1 h of primary characterization, the emissions were photo-oxidized by exposing them to UV lights (model F40BL UVA, General Electric).

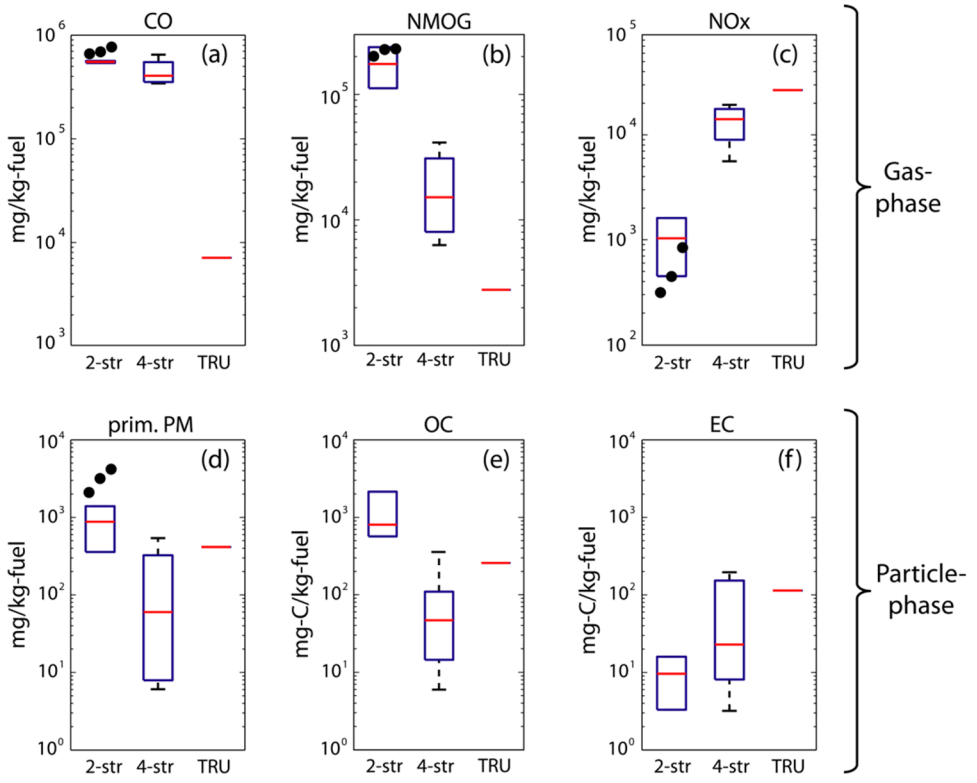

Figure 1. (a)−(c) Gas- and (d)−(f) particle-phase data measured in the CVS for 10 gasoline SORE (six 2-stroke and four 4-stroke) experiments and two TRU experiments. Also shown (black filled circles in panels a−d) are data from a SORE 2-stroke study by Volckens et al.[29] Data from duplicate experiments were averaged before plotting. Only one diesel TRU engine was tested (twice); its values are therefore represented by a single line on the far right side of the six panels. A complete list of all experimental SORE/TRU data (including duplicate experiments) is provided in Table S.5 of the SI. The central marks on the boxplots are medians, the edges of the boxes are the 25th and 75th percentiles and the whiskers extend to the most extreme data points not considered outliers (<1.5× interquartile range).

An array of instruments was used to characterize gas- and particle-phase pollutants inside the chamber. Particle number distributions were measured with a scanning mobility particle sizer (SMPS, TSI, Inc., classifier model 3080, CPC model 3772). Nonrefractory fine PM mass was measured with a quadrupole Aerosol Mass Spectrometer (AMS, HSL experiments) or a high resolution AMS (CMU experiments). Details of the AMS analysis are provided in the SI.

Gas-phase organic species were measured with a proton transfer reaction mass spectrometer (PTR-MS, Ionicon HSL experiments) or a custom built gas chromatography mass spectrometry based system (CMU).[22] Dedicated gas monitors measured CO_2 (LI-820, Li-Cor Biosciences), SO_2, NO_x, CO, and O_3 (API-Teledyne models 100E, 200A, 300A, and 400E); monitors were zeroed daily and calibrated at least weekly. A seven channel Aethalometer (Magee Scientific, model AE-31) measured black carbon (BC), and the Aethalometer attenuation measurements were corrected for particle loading effects using the method of Kirchstetter and Novakov.[23]

Hydroxyl radical (OH) levels in the chamber were inferred from the measured decay of deuterated butanol and other VOCs (e.g., toluene, xylenes, TMB, propene).[24] The butanol provided very clear (little interference from other compounds) OH exposure data and does not form SOA.

The experiments were designed to investigate relatively fresh SOA—similar to what might be formed via gas-phase oxidation in urban environments (modest OH exposures, high NO_x, and moderate organic aerosol concentrations). A summary of selected initial and final chamber conditions is provided in Table S.6 of the SI. Initial POA concentrations inside the chamber ranged from 0.9 to 4 $\mu g/m^3$ for the 2-stroke and from 12.1 to 20 $\mu g/m^3$ for the 4-stroke tests, which span typical urban PM concentrations. This primary PM served as the seed for SOA formation. Typical experiment average OH levels were $3-5 \times 10^6$ molecules cm^{-3}, which is within the range of summer daytime atmospheric concentrations.[25] OH levels were generally higher ($\sim 2 \times 10^7$ molecules cm^{-3}) during the initial stages of the photo-oxidation phase of an experiment and then fell ($\sim 1 \times 10^6$ molecules cm^{-3}) as the HONO was photolyzed. The mixing ratios of individual single-ring aromatics in the chamber were typically less than 20 ppb. Initial NO_x concentrations in the chamber were between 0.2 and 1.8 ppm—much higher than typical urban conditions. Fortunately, SOA yields are thought to be less sensitive to absolute concentrations, especially if the organic aerosol levels in the chamber are atmospherically relevant. To the extent that the product distribution of the organic oxidation reactions differs from the atmosphere, these differences will influence the SOA formation.

The smog chamber was located in a large air conditioned space; the temperature and relative humidity in the chamber varied between 25 and 28 °C and 4−13%. The very low RH means that aqueous SOA formation probably did not occur in these experiments.

Blank experiments were run to assess background levels of gases and particles in the chamber.[18] During the blank experiment CVS air was added to the chamber (no exhaust) as well as ammonium sulfate seed aerosol, HONO and

propene. Blank experiments produced 1−3 $\mu g/m^3$ of SOA over a 3 h photo-oxidation period. This SOA was likely formed from the residual vapors that desorb from the CVS, transfer line and chamber wall. Therefore, for every chamber experiment we assumed an SOA blank of 0 $\mu g/m^3$ at t = 0 that increased linearly to 2 $\mu g/m^3$ of SOA at t = 3 h and subtracted this artifact from the reported SOA production. This correction was much smaller than the SOA formed in experiments with dilute SORE exhaust.

Calculation of Emission Factors. Time-based emissions of gas- and particle-phase species measured in the CVS for multimode tests were calculated using the following relationship[26]

$$\text{emission}_k = \sum_{n}^{i=1} E_i W_i \quad (1)$$

where emission_k is the time-based emission rate for species k (in g/h), E_i is the emission rate in the CVS (in g/h) for mode i of the test cycle, W_i is the weighting factor (SI Table S.3) for mode i of the test cycle and n is the number of modes in the test cycle. The weighting factor is the fraction of time that the engine is expected to be operated in each mode during its lifetime. The emissions data were converted to fuel-based emission factors (grams of species per kilogram fuel consumed) from the measured pollutant concentrations using the carbon mass balance:

$$EF_k = \frac{\text{emission}_k \cdot x_c}{\Delta CO_2 + \Delta CO + \Delta HC}$$

where emission_k is the time-based emission rate for species k in the CVS (in g/h) from eq 1, x_c is the mass fraction of carbon in the fuel (0.85, see Table S.4 of the SI), and ΔCO_2, ΔCO, and ΔHC are the background-corrected carbon concentrations of CO_2, CO and hydrocarbons measured in the CVS (in g-carbon/h). As much as 40% of fuel carbon was emitted as CO and HC; therefore these species must be included in the carbon mass balance.

SOA Wall-loss Corrections. To quantify SOA production, the smog chamber data must be corrected for loss of particles and condensable vapors to the chamber walls. A detailed discussion of these corrections may be found elsewhere.[19] Briefly, the loss of organic particles to the walls is well constrained. It is treated as a first-order process[27] with a rate constant determined from the measured decay of nonreactive PM species (e.g., BC or an inorganic seed). The particle wall-loss rate ranged from 0.25 to 0.55 h^{-1}. This requires that particles be internally mixed; an assumption that was verified with the AMS and SMPS data.

The loss of condensable organic vapors to the walls is more uncertain. We bound it by two limiting cases. Assuming that no organic vapors are lost to the walls or wall-bound particles (first case) provides a lower bound estimate of SOA production, equivalent to the "ω = 0" correction utilized in previous studies.[8,20] Assuming that organic vapors remain in equilibrium with both wall-bound and suspended particles (second case) provides the upper bound, equivalent to the "ω = 1" correction.[8] We do not consider the loss of organic vapors directly to the chamber walls (in distinction to their loss to wall-bound particles).[28] This is highly uncertain; if included, it would *increase* our estimated SOA production.

RESULTS

Primary Emissions. Gas (CO, NO_x, and NMOG) and particle (mass, OC, EC) emissions are summarized in Figure 1. These data are also in Table S.5 of the SI. Comparing emissions data from different engines is complicated by the fact that the engines were tested using different duty cycles (Table S.1 of the SI). For example, half of the 4-strokes were tested using Cycle C and the other half with Cycle A (regulations require that leaf blowers of a certain displacement be tested using Cycle C, regardless of whether they are powered by 2- or 4-stroke engines). The test cycles were designed based on real-world operations; thus, the data should be a reasonable predictor for real-world emissions.

The trends in primary emissions shown in Figure 1 are largely consistent with previous studies.[29] The 2- and 4-stroke gasoline SOREs emitted nearly 2 orders of magnitude more CO (per mass of fuel) than the diesel-powered TRU and about 60 times more than newer light-duty gasoline vehicles (LDGV).[18] The 2-stroke gasoline SOREs had the highest nonmethane organic gas (NMOG) emissions, approximately 3-orders of magnitude higher than the emissions from the newest LDGV.[18] A large fraction of these emissions were likely unburned fuel which mixed with postcombustion products as they were exhausted from the engine cylinder.[29−31] The 4-stroke gasoline SOREs emitted an order of magnitude less NMOG than 2-strokes, but their emissions were still very high relative to LDGV. The TRU emitted much less NMOG than the gasoline SOREs, roughly comparable with uncontrolled (i.e., no aftertreatment) diesel vehicles.[19] The TRU had the highest NO_x emissions followed by the 4-stroke and then the 2-stroke gasoline SOREs. The 2-stroke NO_x emissions were quite low, presumably because these engines operate fuel rich.

Figure 1d indicates that 2-stroke gasoline SOREs emitted the most primary PM—at least an order of magnitude greater than the primary PM from LDGV.[18] Four-stroke gasoline SOREs emitted less primary PM than 2-strokes, and though 4-stroke emission rates were highly variable, the median emissions were comparable to older LDGV.[18] Primary PM emissions from the TRU were similar to those from uncontrolled diesel vehicles.[19]

The PM emissions were predominantly carbonaceous. The median POA emissions (Figure 1e) measured in the CVS were estimated by the difference between the total primary PM and the EC. Direct measurements of POA (via quartz filter) were greater than the primary PM in some experiments due to the adsorption of organic gases to the quartz filter (quartz-behind-Teflon filters were not collected) and partitioning biases induced by the different sampling temperatures for the Teflon and quartz filters. POA from 4-stroke gasoline SOREs was about a factor of 5 lower than the TRU and nearly a factor of 20 lower than the 2-strokes (0.87 g-C/kg-fuel). This trend is unchanged if medians are calculated using only 2-strokes and 4-strokes tested on cycle C (comparison not shown). The much higher POA emissions from the 2-stroke was presumably due to the lubricating oil mixed with the fuel. The 2-strokes emit 1−2 orders of magnitude more POA than LDGV.[18] As expected, the diesel powered TRU emitted roughly an order of magnitude more EC than the gasoline SOREs.[32−34] The emissions of water-soluble anions and cations were very low, contributing, at most 5% of the PM mass. Measurable levels of nitrate, sulfate and potassium were only observed in the SORE2S-2.1 and SORE2S-2.2 experiments. For the other experiments the inorganic ions were below detection limits.

Figure 1 indicates that the NMOG emissions from the gasoline SOREs and TRU were 1−2 orders of magnitude greater than the POA emissions. Therefore, if even a small fraction (a few percent in the case of gasoline SOREs) of the NMOG emissions is converted to SOA, SOA will dominate the SORE contribution to ambient PM. To better understand the SOA formation potential from gas-phase oxidation, Table S.7 of the SI lists emission factors for 203 individual species. Figure 2

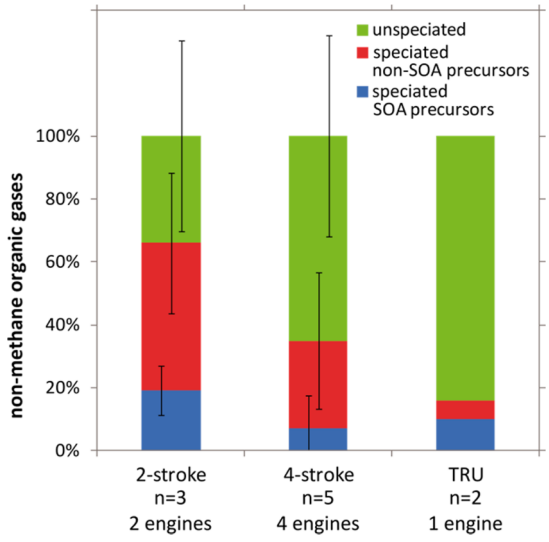

Figure 2. Speciated nonmethane organic gas data sorted based on potential to form SOA from gas-phase oxdiation. Mass fractions ($\pm 1\sigma$) of speciated SOA precursors, speciated non-SOA precursors and unspeciated nonmethane organic gas (NMOG) emissions for 2- and 4-stroke gasoline SORE and diesel TRU. Multiple experiments with the same engine were averaged before plotting. No error bars are shown for the TRU since only a single engine was tested.

summarizes these data by lumping them into three categories based on their potential to form SOA from gas-phase oxdiation: (1) speciated SOA precursors which include single-ring aromatics (C_6 to C_{12}) and midweight hydrocarbons (C_9 to C_{12}); (2) speciated non-SOA precursor which include non-aromatic carbonyls (C_1 to C_8) and low molecular weight hydrocarbons (C_2 to C_8); and (3) unspeciated NMOG—defined as the difference between the total NMOG as measured with the flame ionization detector and the sum of speciated mass. This unspeciated NMOG is presumed to be a combination of high molecular weight hydrocarbons and oxygenates which were not classified by the GC-based speciation techniques. Speciated SOA precursors contribute 10−20% of the total NMOG emissions, while unspeciated organics contribute another 30−80% of the NMOG mass.

Duplicate experiments were performed with five of the seven engines. The variability in CVS emissions between duplicate experiments was generally small (Table S.5 of the SI). For example, the maximum differences between pairs of NMOG measurements and pairs of CO measurements in the five sets of duplicate experiments were 6% and 11%, respectively. Excellent agreement (~ ±5%) was also observed between duplicate experiments for primary PM for four of the five engines; the SORE4S-2 experiments were somewhat more variable.

Secondary Organic Aerosol Production. Figure 3 plots the time series of particle- and gas-phase species measured during a typical smog chamber experiment (SORE2S-1.1).

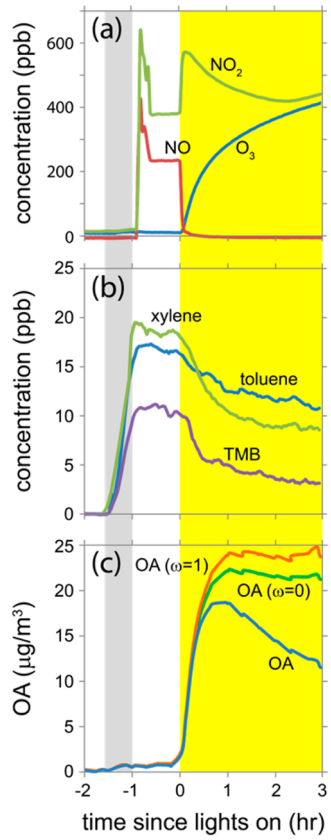

Figure 3. Gas and particle evolution during a typical smog chamber experiment (SORE2S-1.1). Between −1.4 h < time < −1.0 h, the chamber was filled with dilute emissions from the backpack blower; for −1.0 h < time <0 h, the primary PM was characterized; for time >0 h, the UV lights were on and photo-oxidation generated SOA. Concentrations of NO, NO_2, and O_3 are shown in (a). Shown in (b) are the concentrations of three VOCs which are consumed by OH radicals during the photo-oxidation period (TMB = trimethylbenzene). Shown in (c) are uncorrected and corrected (for wall-losses) organic PM concentrations; the large increase is due to SOA production. The organic concentrations were corrected using two different methods (ω = 0 and ω =1) which provide an estimate of the uncertainty of the SOA production.

There are three distinct periods in each experiment. First, emissions were added to the chamber causing pollutant concentrations to increase. The second period began when the engine was shut off (~ −1 h in Figure 3). During this period the primary emissions were characterized and HONO and propene were added to the chamber. HONO was added to the chamber at ~ −0.9 h, increasing the NO_2 concentration. The third period began when the UV lights were turned on (0 h). During the 3 h of UV irradiation much of the NO and primary hydrocarbons were oxidized to NO_2 and oxygenated VOCs, respectively (Figure 3a,b). There was also rapid and substantial production of SOA, with the suspended organic aerosol concentration increasing from 1 to 17 $\mu g/m^3$ after the first half an hour of UV exposure. After 3 h of photo-oxidation the wall-loss corrected organic aerosol concentrations had increased by roughly a factor of 20 from ~1 $\mu g/m^3$ of POA to ~22 $\mu g/m^3$ of mainly SOA (average of the ω = 0 and ω = 1 estimates in Figure 3c).

Although the NO_x levels in the chamber were very high, Figure 3a indicates that the NO levels fell to below a few ppbv (the limit of detection) after about thirty minutes of photo-

dx.doi.org/10.1021/es403556e | Environ. Sci. Technol. 2013, 47, 14137−14146

oxidation. This occurred in three of the 2-stroke experiments; in the other experiments NO levels were always greater than 100 pbbv. Thus, during the latter experiments the chemistry in the chamber probably shifted from a high- to a low-NO_x regime because the fate of the organoperoxy radicals (RO_2) depends on NO concentrations. If substantial NO is present, then RO_2 + NO reactions dominate, creating "high NO_x conditions"; at very low NO levels, RO_2 + HO_2 and RO_2 + RO_2 reactions will dominate creating "low NOx conditions." Therefore, in experiments in which NO levels fell to very low levels (e.g., Figure 3c), the SOA formation was influenced by both high and low NO_x chemistry.

Although Figure 3c indicates that NO levels dropped below a few ppbv after ~30 min of photo-oxidation, it is not clear that the SOA formation was dominated by low-NO_x reactions. First, the majority of the SOA formation occurred in the first part of the experiment when there was still NO in the chamber. For example, for the experiment in Figure 3, it took about 30 min for the NO to fall to ~0. During this time about 75% of the SOA formation occurred. Second, the UV lights were kept on throughout the photochemical oxidation phase of the experiment, which continuously generated NO via the photolysis of NO_2. Third, the O_3 and NO_2 in the chamber increased monotonically throughout every experiment, even those in which NO fell to ~0. Therefore, in every experiment some of the RO_2 must have reacted with NO, even when the NO levels were very low. Fourth, the AMS measured substantial particle-phase organic nitrate in every experiment. Therefore, it is clear that the high NO_x pathway was important in every experiment. However, the complexity of the chemistry inside the chamber makes it difficult to quantitatively assess the relative importance of the high- and low-NO_x pathways in the experiments in which NO levels fell to a few ppbv.

The AMS mass spectra of the SOA formed in the chamber were similar to ambient data.[35] For the 2- (4-) stroke experiments the O/C ratio increased from 0.1 to 0.5 (0.3) within the first 15 min of photo-oxidation and then remained essentially constant. Both the 2- and 4-stroke O/C values are similar to semivolatile oxygenated organic aerosol (SV-OOA) factors derived from ambient data collected in a large number of urban environments.[36]

The SOA production measured after 3 h of photo-oxidation from the six SORE chamber experiments is plotted in Figure 4 along with the ratio of SOA to primary PM (data are in Tables S.5 and S.6 of the SI). Median SOA produced from 2-stroke gas-phase emissions were a factor of 7−8 greater than that from the 4-stroke. This is likely due to the much higher NMOG emissions and lubrication oil contribution (Figure 1). After three hours of photo-oxidation, there was about twice as much SOA as primary PM in the CVS for the 2-stroke experiments. By the end of the 4-stroke experiments, the SOA production was equal to about 20% of the primary PM in the CVS. The fact that the absolute amount of 2-stroke primary PM was so high underscores just how much SOA may originate from these engines' emissions.

Although the SOA experiments were performed using one 2-stroke engine and one 4-stroke engine, Figure 4 indicates that there was significant experiment-to-experiment variability in the SOA production. SOA formation depends on the precursor concentrations, gas-particle partitioning, oxidant exposure, and VOC/NO_x. Presenting the data on a fuel basis accounts for differences in chamber precursor concentrations due to the

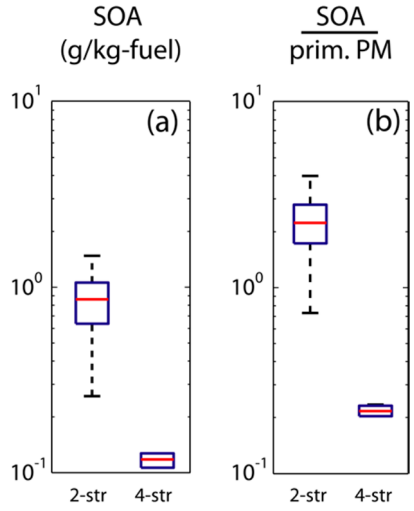

Figure 4. Particle-phase data for four experiments with SORE2S-1 and 3 experiments with SORE4S-4. (a) secondary organic aerosol measured in the chamber, and (b) ratio of SOA to total primary PM mass from gravimetric analysis of Teflon filters collected in the CVS following CFR 1065 procedures. Although SOA is quantified using the same units as the primary PM emission factor, the reported SOA production pertains to the sampled experimental conditions only and should not be considered an emission factor. Note that the primary emissions used to construct these plots are based on a subset of the data shown in Figure 1. Data from duplicate experiments were averaged before plotting. The central marks on the boxplots are medians, the edges of the boxes are the 25th and 75th percentiles and the whiskers extend to the most extreme data points.

modest experiment-to-experiment variability in NMOG emissions.

There were large experiment-to-experiment differences in organic aerosol concentration (C_{oa}) due to technical challenges of injecting the same amount of exhaust into the chamber. To investigate whether the varying C_{oa} influenced SOA production via gas-particle partitioning Figure S.2 in the SI presents the end-of-experiment SOA data in a partitioning plot.[37] SOA production increased monotonically with C_{oa} inside the chamber, suggesting that the SOA is semivolatile.[37,38] This behavior is commonly observed in smog chamber experiments performed with single precursors.[39,40] SI Figure S.2 indicates that, at a given C_{OA}, the SOA production in the two-stroke SORE experiments was dramatically higher than in the four-stroke experiments. Therefore, the large differences between the two- and four-stroke SOA production was not due to partitioning effects.

In addition to C_{OA}, two other factors also likely contributed to the experiment-to-experiment variability in the SOA production. First, individual OH exposures varied by about a factor of 2 across the set of experiments (except for SORE2S-1.1 which was about a factor five greater). Second, in some of the two-stroke experiments the chemistry transitioned from high- to a low-NO_x regime. Although this can influence SOA yields,[41] its effect is unlikely to be large enough to explain the differences between 2- and 4-stroke sources shown in Figure 4.

We calculated an effective yield to characterize the SOA formation potential of the emissions. An effective yield is the ratio of the SOA mass to the sum of the SOA precursor mass consumed during photo-oxidation. It quantifies the fraction of the precursor mass that must be converted to SOA in order to explain the chamber data. We use the term "effective" yield

because combustion emissions comprise a complex mix of species of which only a subset were quantified by the GC analysis.

The effective yield calculation is described in more detail elsewhere.[18] We performed the effective yield analysis accounting for the reaction of speciated SOA precursors (single-ring aromatics (C_6 to C_{12}) and midweight hydrocarbons (C_9 to C_{12}) (see SI)) and unspeciated NMOG. The changes in the concentrations of each of the speciated precursors were calculated from their initial concentration (inferred from the CVS data), the OH exposure and the reaction rate of that species with OH. The unspeciated NMOG were treated as a single lumped species that was assumed to react at 2×10^{-11} cm^3 $molecule^{-1}$ s^{-1}.[42] Multiplying or dividing this reaction rate by a factor of 2 has a negligible effect on the results, changing the yields by <1%.

Figure 5 plots the effective yields calculated for three gasoline SORE experiments conducted at HSL. These yields account for the reaction of both speciated SOA precursors and unspeciated NMOG. The effective yields of the dilute gasoline SORE exhaust ranged from 2 to 4%, which overlaps the SOA yields for unburned gasoline[43] and emissions from older (pre-LEV) LDGVs.[18] This suggests that much of the SOA production may be driven by emissions of unburned fuel and/or lubrication oil. Exhaust from the 2- and 4-stroke SORES had similar SOA yields even though there are substantial differences in NMOG speciation profiles (Figure 2).

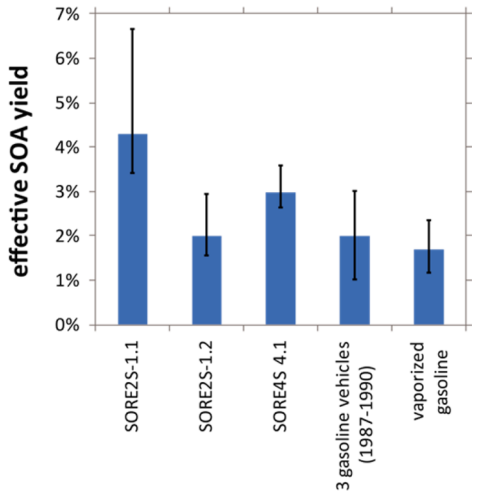

Figure 5. Estimated effective SOA yields accounting for the oxidation of speciated SOA precursors and unspeciated NMOGs for the three SORE chamber experiments performed at HSL compared to median SOA yields for unburned gasoline[43] and from the emissions of 3 different older gasoline vehicles.[18] The error bars for the SORE represent the range of yield values obtained when the OH exposure is varied by $\pm 1\sigma$. The unburned gasoline error bar represents the range of values measured for 1 $\mu g\ m^{-3} < C_{oa} < 10\ \mu g\ m^{-3}$. The gasoline vehicle error bar represents the standard deviation from five separate experiments with the three vehicles.

Assuming only known SOA precursors reacted (no SOA formation from unspeciated NMOG) results in slightly higher effective yields—8%, 3%, and 5% (data not shown) for the SORE2S-1.1 and SORE2S-1.2 and SORE4S-4.1 experiments, respectively. The greater increase in effective yield for the SORE2S-1.1 experiment—4% (8%) with (without) unspeciated NMOG—as compared to the SORE2S-1.2 duplicate experiment—2% (3%) with (without) unspeciated NMOG—is due to the fact that the OH exposure was about a factor of 2 greater in the former experiment than in the latter. The difference in OH exposure also explains the greater effective yield for the SORE2S-1.1 experiment (4%) versus the SORE2S-1.2 experiment (2%).

DISCUSSION

To develop effective air pollution control strategies one must understand the overall contribution of emissions from mobile sources to ambient PM—both primary particle emissions and secondary PM formed in the atmosphere. The median primary PM (i.e., EC+POA) and SOA data from the SORE experiments are summarized in Figure 6a along with data from on-road gasoline and diesel vehicles conducted using the same experimental techniques.[18,19] The total height of each bar in Figure 6a indicates the quantity of the three different types of PM (EC and POA measured in the CVS and SOA measured in the smog chamber) after three hours of photo-oxidation. The data are presented relative to the fuel consumed to facilitate consistent comparisons between the different emission sources. SOA production in the atmosphere depends on many variables (e.g., [OH], relative humidity, VOC:NO_x etc.). Therefore, the data in Figure 6 correspond to the conditions of our experiments. The SOA values should not be considered emission factors.

For the set of mobile sources tested during this project, Figure 6a indicates that 2-stroke gasoline SOREs contributed the most PM in the chamber relative to their fuel consumption. The 2-stroke gasoline SOREs had both high primary PM emissions (mainly POA) as well as the most SOA formation. Accounting for both primary PM and SOA, Figure 6a indicates that 2-stroke SOREs contributed about 30 times more PM (per mass of fuel consumed) than modern gasoline vehicles (LEV I and LEV II) and about 14 times more than light-duty gasoline vehicles manufactured 20 years ago (pre-LEV). The net contribution of 4-stroke SOREs was about a factor of 10 less than 2-stroke SOREs but still higher than older (pre-LEV) on-road vehicles and 3−4 times greater than newer LDGV. Thus, as regulations for on-road gasoline vehicles have reduced their contribution to ambient PM over the last several decades, the role of SOREs has become increasingly important.

Uncontrolled (no diesel particulate filter) diesel vehicles comprise the only source class with a comparable amount (although still substantially less) of PM as the SOREs. Uncontrolled diesels emitted high levels of primary PM (mainly EC), while SOA was relatively more important for the gasoline powered SOREs, especially the 2-stroke SOREs. The substantial SOA production from dilute gasoline SORE exhaust is not surprising in light of their very high NMOG emissions.

These experiments only photochemically aged the diluted exhaust for three hours, which is much less than what will occur in the atmosphere. Field studies have shown that SOA production downwind of urban areas may persist for 48 h.[44,45] Although the SOA production rate decreased as an experiment progressed, this appeared to be largely due to the decrease in oxidant rather than SOA precursor concentrations; therefore, the smog chamber data we present may underestimate the ultimate production of SOA from dilute exhaust in the atmosphere. If so, SOREs may be responsible for an even larger contribution to ambient PM (where there is excess OH) than is suggested by Figure 6. In addition, the low humidity in

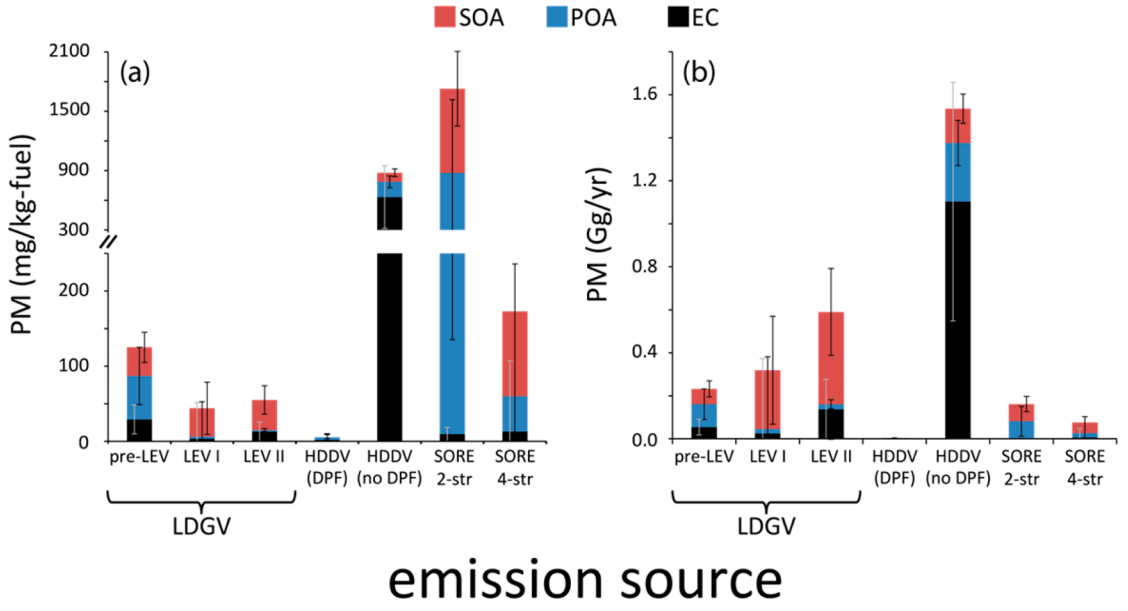

Figure 6. (a) Median EC and POA emissions (measured in the CVS) and SOA production from gasoline small off-road engines (SOREs), light-duty gasoline vehicles (LDGVs) and heavy-duty diesel vehicles (HDDVs), and (b) estimated source contributions to the atmospheric PM burden in the Los Angeles area. LDGV data were obtained during cold-start Unified Cycle experiments with a single CA summertime gasoline.[18] There are three types of LDGV: pre-LEV vehicles were manufactured before 1995; LEV I vehicles were manufactured between 1995 and 2003; and LEV II vehicles were manufactured after 2003. HDDV data were obtained during Urban Dynamometer Driving Schedule (UDDS) driving cycle experiments with three different types of ULSD fuel.[19] The HDDVs were either equipped with a diesel particulate filter (DPF) or no exhaust aftertreatment (no DPF). Median SOA values were calculated from the averages obtained by applying the $\omega = 0$ and $\omega = 1$ wall-loss correction approaches. Error bars represent $\pm 1\sigma$. The absence of error bars for several of the SORE measurements is due to limited data for these sources.

these chamber experiments obviated aqueous SOA production, thereby further underestimating the potential impact of these sources.

Figure 6 indicates that vehicles equipped with diesel particulate filters had the lowest contribution of any of the mobile sources tested during this project. They had both very low primary PM emissions as well as negligible SOA formation. Therefore, catalyzed diesel particulate filters appear to be a very effective emissions control technology.

Figure 6b shows the PM emissions and SOA production data scaled by fuel consumption in the South Coast Air Basin of California (Los Angeles, Riverside, Orange, and San Bernardino counties in 2010) to estimate the potential contribution of these different source categories to the atmospheric PM burden. Fuel consumption was calculated using CARB's EMFAC[46] and OFFROAD[47] models; these data are listed in Table S.8 of the SI.

Figure 6 shows that although the SORE PM contribution is very large relative to the amount of fuel they consume, their overall contribution to the atmosphere is still small compared to on-road vehicles, which consume a dominate share of the fuel. About 8% of the mobile source-derived PM (excluding off-road diesels and commercial air, rail and marine vessels) in the South Coast Air Basin may be attributed to combustion emissions from 2- and 4-stroke SOREs. This is smaller than any on-road vehicle category except for heavy-duty diesel vehicles equipped with particle filters. Nevertheless, as an increasingly large share of the diesel vehicle fleet is equipped with these filters, our results suggest that the importance of SOREs will grow dramatically. Figure 6b suggests that as the HDDV (no DPF) category is eliminated (due to policy passed in 2007 requiring DPFs on all new HDDVs) the SORE PM fraction could increase by a factor of 2 or more.

■ ASSOCIATED CONTENT

Supporting Information

Tables of emissions data and additional figures are available free of charge via the Internet at http://pubs.acs.org/

■ AUTHOR INFORMATION

Corresponding Author

*(A.L.R.) E-mail: alr@andrew.cmu.edu.

Present Address

○National Oceanic and Atmospheric Administration Earth System Research Laboratory, Chemical Sciences Division, 325 Broadway, Boulder, Colorado 80304 and Cooperative Institute for Research in Environmental Sciences, University of Colorado, 216 UCB, Boulder, Colorado 80309.

Notes

The authors declare no competing financial interest.

■ ACKNOWLEDGMENTS

This research would not have been possible without the hard work of the excellent and dedicated staff at the California Air Resources Board's Haagen-Smit Laboratory. Funding was provided by the U.S. Environmental Protection Agency National Center for Environmental Research (NCER) through the STAR program (R834554) and the Coordinating Research Council through Project No. A-74/E-96. The California Air Resources Board provided significant in-kind support for the testing. The National Science Foundation provided support through its Graduate Research Fellowship Program. While this article is believed to contain correct information, Ford Motor Company (Ford) does not expressly or impliedly warrant, nor assume any responsibility, for the accuracy, completeness, or usefulness of any information, apparatus, product, or process disclosed, nor represent that its use would not infringe the

rights of third parties. Reference to any commercial product or process does not constitute its endorsement. This article does not provide financial, safety, medical, consumer product, or public policy advice or recommendation. Readers should independently replicate all experiments, calculations, and results. The views and opinions expressed are of the authors and do not necessarily reflect those of Ford. This disclaimer may not be removed, altered, superseded or modified without prior Ford permission.

REFERENCES

(1) Davis, S. C.; Diegel, S. W.; Boundy, R. G. *Transportation Energy Data Book*, 32nd ed.;. United States Department of Energy, 2013.

(2) U.S. EPA OAQPS. *Regulatory Announcement. Final Phase 2 Standards for Small, Spark-Ignitioned Handheld Engines*, EPA-420-F-00-007; U.S. Environmental Protection Agency, 2000.

(3) Volckens, J.; Olson, D. A.; Hays, M. D. Carbonaceous species emitted from handheld two-stroke engines. *Atmos. Environ.* **2008**, *42* (6), 1239−1248.

(4) Jimenez, J. L.; Canagaratna, M. R.; Donahue, N. M.; Prevot, A. S. H.; Zhang, Q.; et al. Evolution of organic aerosols in the atmosphere. *Science* **2009**, *326* (5959), 1525−1529.

(5) Subramanian, R.; Donahue, N. M.; Bernardo-Bricker, A.; Rogge, W. F.; Robinson, A. L. Insights into the primary-secondary and regional-local contributions to organic aerosol and $PM_{2.5}$ mass in Pittsburgh, Pennsylvania. *Atmos. Environ.* **2007**, *41* (35), 7414−7433.

(6) Stone, E. A.; Zhou, J.; Snyder, D. C.; Rutter, A. P.; Mieritz, M.; Schauer, J. J. A comparison of summertime secondary organic aerosol source contributions at contrasting urban locations. *Environ. Sci. Technol.* **2009**, *43* (10), 3448−3454.

(7) Nakao, S.; Shrivastava, M.; Nguyen, A.; Jung, H.; Cocker, D., III Interpretation of secondary organic aerosol formation from diesel exhaust photooxidation in an environmental chamber. *Aerosol Sci. Technol.* **2011**, *45* (8), 964−972.

(8) Weitkamp, E.; Sage, A.; Pierce, J.; Donahue, N.; Robinson, A. Organic aerosol formation from photochemical oxidation of diesel exhaust in a smog chamber. *Environ. Sci. Technol.* **2007**, *41* (20), 6969−6975.

(9) Hung, H. F.; Wang, C. S. Formation of secondary organic aerosols and reactive oxygen species from diluted motorcycle exhaust. *J. Chin. Inst. Chem. Eng.* **2006**, *37* (5), 491−499.

(10) McWhinney, R. D.; Gao, S. S.; Zhou, S.; Abbatt, J. P. Evaluation of the effects of ozone oxidation on redox-cycling activity of two-stroke engine exhaust particles. *Environ. Sci. Technol.* **2011**, *45* (6), 2131−2136.

(11) Ervens, B.; Feingold, G.; Frost, G. J.; Kreidenweis, S. M. A modeling study of aqueous production of dicarboxylic acids: 1. Chemical pathways and speciated organic mass production. *J. Geophys. Res., [Atmos.]* **2004**, *109* (D15), D15205.

(12) Gelencser, A.; Varga, Z. Evaluation of the atmospheric significance of multiphase reactions in atmospheric secondary organic aerosol formation. *Atmos. Chem. Phys.* **2005**, *5*, 2823−2831.

(13) Lim, Y.; Tan, Y.; Perri, M.; Seitzinger, S.; Turpin, B. Aqueous chemistry and its role in secondary organic aerosol (SOA) formation. *Atmos. Chem. Phys.* **2010**, *10* (21), 10521−10539.

(14) Carlton, A.; Turpin, B. Particle partitioning potential of organic compounds is highest in the Eastern US and driven by anthropogenic water. *Atmos. Chem. Phys.* **2013**, *13*, 10203−10214.

(15) May, A. A.; Nguyen, N. T.; Presto, A. A.; Gordon, T. D.; Lipsky, E. M.; Karve, M.; Gutierrez, A.; Robertson, W. H.; Zhang, M.; Chang, O.; Chen, S.; Cicero-Fernandez, P.; Fuentes, M.; Huang, S.; Ling, R.; Long, J.; Maddox, C.; Massetti, J.; McCauley, E.; Na, K.; Pang, Y.; Rieger, P.; Sax, T.; Truong, T.; Vo, T.; Chattopadhyay, S.; Maldonado, H.; Maricq, M. M.; Robinsonm A. L. Gas- and particle-phase primary emissions from in-use, on-road gasoline and diesel vehicles. *Atmos. Environ.*, **2013**, submitted.

(16) May, A. A.; Presto, A. A.; Hennigan, C. J.; Nguyen, N. T.; Gordon, T. D.; Robinson, A. L. Gas-particle partitioning of primary organic aerosol emissions: (1) Gasoline vehicle exhaust. *Atmos. Environ.* **2013**, *77* (0), 128−139.

(17) May, A. A.; Presto, A. A.; Hennigan, C. J.; Nguyen, N. T.; Gordon, T. D.; Robinson, A. L. Gas-particle partitioning of primary organic aerosol emissions: (2) Diesel vehicles. *Environ. Sci. Technol.* **2013**, *47* (15), 8288−8296.

(18) Gordon, T. D.; Presto, A. A.; May, A. A.; Nguyen, N. T.; Lipsky, E. M.; Donahue, N. M.; Gutierrez, A.; Zhang, M.; Maddox, C.; Rieger, P.; Chattopadhyay, S.; Maldonado, H.; Maricq, M. M.; Robinson, A. L. Secondary organic aerosol formation exceeds primary particulate matter emissions for light-duty gasoline vehicles. *Atmos. Chem. Phys. Discuss.* **2013**, *13*, 23173−23216.

(19) Gordon, T. D.; Presto, A. A.; Nguyen, N. T.; Robertson, W. H.; Na, K.; Sahay, M.; Zhang, M.; Maddox, C.; Rieger, P.; Chattopadhyay, S.; Maldonado, H.; Maricq, M.; Robinson, A. L. Secondary organic aerosol production from diesel vehicle exhaust: Impact of aftertreatment, fuel chemistry and driving cycle. *Atmos. Chem. Phys. Discuss.* **2013**, *13*, 24223−24262.

(20) Miracolo, M.; Hennigan, C.; Ranjan, M.; Nguyen, N.; Gordon, T.; Lipsky, E.; Presto, A.; Donahue, N.; Robinson, A. Secondary aerosol formation from photochemical aging of aircraft exhaust in a smog chamber. *Atmos. Chem. Phys.* **2011**, *11*, 4135−4147.

(21) Grieshop, A.; Logue, J.; Donahue, N.; Robinson, A. Laboratory investigation of photochemical oxidation of organic aerosol from wood fires 1: Measurement and simulation of organic aerosol evolution. *Atmos. Chem. Phys.* **2009**, *9*, 1263−1277.

(22) Logue, J.; Huff-Hartz, K.; Lambe, A.; Donahue, N.; Robinson, A. High time-resolved measurements of organic air toxics in different source regimes. *Atmos. Environ.* **2009**, *43* (39), 6205−6217.

(23) Kirchstetter, T. W.; Novakov, T. Controlled generation of black carbon particles from a diffusion flame and applications in evaluating black carbon measurement methods. *Atmos. Environ.* **2007**, *41* (9), 1874−1888.

(24) Atkinson, R.; Arey, J. Atmospheric degradation of volatile organic compounds. *Chem. Rev.* **2003**, *103* (12), 4605−4638.

(25) Seinfeld, J.; Pandis, S. N. *Atmospheric Chemistry and Physics: From Air Pollution to Climate Change*; John Wiley & Sons, Inc.: Hoboken, NJ, 2006

(26) California Air Resources Board, California Exhaust Emission Standards and Test Procedures for 1995−2004 and Later Small Off-Road Engines. In http://www.arb.ca.gov/regact/sore/test_fin.pdf, 1999.

(27) McMurry, P. H.; Grosjean, D. Gas and aerosol wall losses in Teflon film smog chambers. *Environ. Sci. Technol.* **1985**, *19* (12), 1176−1182.

(28) Matsunaga, A.; Ziemann ‡, P. J. Gas-wall partitioning of organic compounds in a teflon film chamber and potential effects on reaction product and aerosol yield measurements. *Aerosol Sci. Technol.* **2010**, *44* (10), 881−892.

(29) Volckens, J.; Braddock, J.; Snow, R. F.; Crews, W. Emissions profile from new and in-use handheld, 2-stroke engines. *Atmos. Environ.* **2007**, *41* (3), 640−649.

(30) Kado, N. Y.; Okamoto, R. A.; Karim, J.; Kuzmicky, P. A. Airborne particle emissions from 2- and 4-stroke outboard marine engines: Polycyclic aromatic hydrocarbon and bioassay analyses. *Environ. Sci. Technol.* **2000**, *34* (13), 2714−2720.

(31) Yang, H.-H.; Hsieh, L.-T.; Liu, H.-C.; Mi, H.-H. Polycyclic aromatic hydrocarbon emissions from motorcycles. *Atmos. Environ.* **2005**, *39* (1), 17−25.

(32) Fujita, E. M.; Campbell, D. E.; Arnott, W. P.; Chow, J. C.; Zielinska, B. Evaluations of the chemical mass balance method for determining contributions of gasoline and diesel exhaust to ambient carbonaceous aerosols. *J. Air Waste Manage. Assoc.* **2007**, *57* (6), 721−740.

(33) Lloyd, A.; Cackette, T. Diesel engines: Environmental impact and control. *J. Air Waste Manage. Assoc.* **2001**, *51* (6), 809−847.

(34) Miracolo, M. A.; Drozd, G. T.; Jathar, S. H.; Presto, A. A.; Lipsky, E. M.; Corporan, E.; Robinson, A. L. Fuel composition and secondary organic aerosol formation: Gas-turbine exhaust and

alternative aviation fuels. *Environ. Sci. Technol.* **2012**, *46* (15), 8493−8501.
(35) Aiken, A. C.; DeCarlo, P. F.; Kroll, J. H.; Worsnop, D. R.; Huffman, J. A.; Docherty, K. S.; Ulbrich, I. M.; Mohr, C.; Kimmel, J. R.; Sueper, D.; Sun, Y.; Zhang, Q.; Trimborn, A.; Northway, M.; Ziemann, P. J.; Canagaratna, M. R.; Onasch, T. B.; Alfarra, M. R.; Prevot, A. S. H.; Dommen, J.; Duplissy, J.; Metzger, A.; Baltensperger, U.; Jimenez, J. L. O/C and OM/OC ratios of primary, secondary, and ambient organic aerosols with high-resolution time-of-flight aerosol mass spectrometry. *Environ. Sci. Technol.* **2008**, *42* (12), 4478−4485.
(36) Ng, N.; Canagaratna, M.; Zhang, Q.; Jimenez, J.; Tian, J.; Ulbrich, I.; Kroll, J.; Docherty, K.; Chhabra, P.; Bahreini, R. Organic aerosol components observed in northern hemispheric datasets from aerosol mass spectrometry. *Atmos. Chem. Phys.* **2010**, *10*, 4625−4641.
(37) Odum, J. R.; Hoffmann, T.; Bowman, F.; Collins, D.; Flagan, R. C.; Seinfeld, J. H. Gas/particle partitioning and secondary organic aerosol yields. *Environ. Sci. Technol.* **1996**, *30* (8), 2580−2585.
(38) Liang, C.; Pankow, J. F.; Odum, J. R.; Seinfeld, J. H. Gas/particle partitioning of semivolatile organic compounds to model inorganic, organic, and ambient smog aerosols. *Environ. Sci. Technol.* **1997**, *31* (11), 3086−3092.
(39) Donahue, N.; Robinson, A.; Stanier, C.; Pandis, S. Coupled partitioning, dilution, and chemical aging of semivolatile organics. *Environ. Sci. Technol.* **2006**, *40* (8), 2635−2643.
(40) Grieshop, A. P.; Miracolo, M. A.; Donahue, N. M.; Robinson, A. L. Constraining the volatility distribution and gas-particle partitioning of combustion aerosols using isothermal dilution and thermodenuder measurements. *Environ. Sci. Technol.* **2009**, *43* (13), 4750−4756.
(41) Kroll, J. H.; Seinfeld, J. H. Chemistry of secondary organic aerosol: Formation and evolution of low-volatility organics in the atmosphere. *Atmos. Environ.* **2008**, *42* (16), 3593−3624.
(42) Jathar, S. H., Gordon, T. D., Hennigan, C. J., Pye, H. O. T., Adams, P. J., Donahue, N. M., and Robinson, A. L., Unspeciated organic emissions from combustion sources and their influence on the secondary organic aerosol budget in the United States. in preparation.
(43) Jathar, S. H.; Miracolo, M. A.; Tkacik, D. S.; Donahue, N. M.; Adams, P. J.; Robinson, A. L. Secondary organic aerosol from photo-oxidation of evaporated fuel: Experimental results and implications for aerosol formation from combustion emissions. *Environ. Sci. Technol.* **2013**, submitted.
(44) de Gouw, J.; Brock, C.; Atlas, E.; Bates, T.; Fehsenfeld, F.; Goldan, P.; Holloway, J.; Kuster, W.; Lerner, B.; Matthew, B. Sources of particulate matter in the northeastern United States in summer: 1. Direct emissions and secondary formation of organic matter in urban plumes. *J. Geophys. Res* **2008**, *113*, D08301.
(45) de Gouw, J. A.; Middlebrook, A. M.; Warneke, C.; Goldan, P. D.; Kuster, W. C.; Roberts, J. M.; Fehsenfeld, F. C.; Worsnop, D. R.; Canagaratna, M. R.; Pszenny, A. A. P.; Keene, W. C.; Marchewka, M.; Bertman, S. B.; Bates, T. S. Budget of organic carbon in a polluted atmosphere: Results from the New England Air Quality Study in 2002. *J. Geophys. Res.* **2005**, *110* (D16), D16305.
(46) California Air Resources Board Motor Vehicle Emission Factor/Emission Inventory Model, EMFAC2011. (June 2013),
(47) California Air Resources Board, User's Guide for OFF-ROAD2007. In http://www.arb.ca.gov/msei/offroad/offroad.htm, 2007.